ESAIM: COCV 18 (2012) 157–180
DOI: 10.1051/cocv/2010049

ESAIM: Control, Optimisation and Calculus of Variations
www.esaim-cocv.org

ON A BERNOULLI PROBLEM WITH GEOMETRIC CONSTRAINTS

Antoine Laurain[1] and Yannick Privat[2]

Abstract. A Bernoulli free boundary problem with geometrical constraints is studied. The domain Ω is constrained to lie in the half space determined by $x_1 \geq 0$ and its boundary to contain a segment of the hyperplane $\{x_1 = 0\}$ where non-homogeneous Dirichlet conditions are imposed. We are then looking for the solution of a partial differential equation satisfying a Dirichlet and a Neumann boundary condition simultaneously on the free boundary. The existence and uniqueness of a solution have already been addressed and this paper is devoted first to the study of geometric and asymptotic properties of the solution and then to the numerical treatment of the problem using a shape optimization formulation. The major difficulty and originality of this paper lies in the treatment of the geometric constraints.

Mathematics Subject Classification. 49J10, 35J25, 35N05, 65P05.

Received March 11, 2010. Revised July 18, 2010 and September 16, 2010.
Published online December 2, 2010.

1. Introduction

Let $(0, x_1, ..., x_N)$ be a system of Cartesian coordinates in $\mathbb{R}^N$ with $N \geq 2$. We set $\mathbb{R}^N_+ = \{\mathbb{R}^N : x_1 > 0\}$. Let K be a smooth, bounded and convex set such that K is included in the hyperplane $\{x_1 = 0\}$. We define a set of *admissible shapes* $\mathcal{O}$ as

$$\mathcal{O} = \{\Omega \text{ open and convex}, K \subset \partial\Omega\}.$$

We are looking for a domain $\Omega \in \mathcal{O}$, and for a function $u : \Omega \to \mathbb{R}$ such that the following over-determined system

$$-\Delta u = 0 \quad \text{in } \Omega, \tag{1.1}$$
$$u = 1 \quad \text{on } K, \tag{1.2}$$
$$u = 0 \quad \text{on } \partial\Omega \setminus K, \tag{1.3}$$
$$|\nabla u| = 1 \quad \text{on } \Gamma := (\partial\Omega \setminus K) \cap \mathbb{R}^N_+ \tag{1.4}$$

has a solution; see Figure 1 for a sketch of the geometry. Problem (1.1)–(1.4) is a *free boundary problem* in the sense that it admits a solution only for particular geometries of the domain Ω. The set Γ is the so-called *free*

Keywords and phrases. Free boundary problem, Bernoulli condition, shape optimization.

[1] Karl-Franzens-University of Graz, Department of Mathematics and Scientific Computing, Heinrichstrasse 36, 8010 Graz, Austria. Antoine.Laurain@uni-graz.at

[2] IRMAR, ENS Cachan Bretagne, Univ. Rennes 1, CNRS, UEB, av. Robert Schuman, 35170 Bruz, France. Yannick.Privat@bretagne.ens-cachan.fr

Article published by EDP Sciences

© EDP Sciences, SMAI 2010

https://doi.org/10.1051/cocv/2010049 Published online by Cambridge University Press

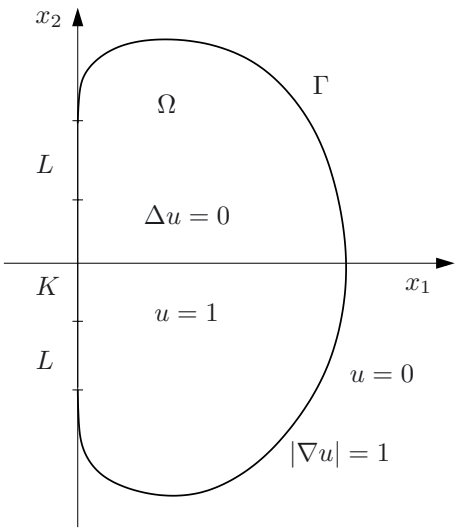


FIGURE 1. The domain Ω in dimension two.

boundary we are looking for. Therefore, the problem is formulated as

$$(\mathcal{F}): \text{ Find } \Omega \in \mathcal{O} \text{ such that problem (1.1)}-\text{(1.4) has a solution.} \tag{1.5}$$

This problem arises from various areas, for instance shape optimization, fluid dynamics, electrochemistry and electromagnetics, as explained in [1,8,10,11]. For applications in N diffusion, we refer to [26] and for the deformation plasticity see [2].

For our purposes it is convenient to introduce the set $L := (\partial\Omega \setminus K) \cap \{x_1 = 0\}$. Problems of the type $(\mathcal{F})$ may or may not, in general, have solutions, but it was already proved in [24] that there exists a unique solution to $(\mathcal{F})$ in the class $\mathcal{O}$. Further we will denote $\Omega^\star$ this solution. In addition, it is shown in [24] that $\partial\Omega^\star$ is $C^{2+\alpha}$ for any $0 < \alpha < 1$, that the free boundary $\partial\Omega^\star \setminus K$ meets the fixed boundary K tangentially and that $L^\star = (\partial\Omega^\star \setminus K) \cap \{x_1 = 0\}$ is not empty.

In the literature, much attention has been devoted to the Bernoulli problem in the geometric configuration where the boundary $\partial\Omega$ is composed of two connected components and such that Ω is connected but not simply connected (for instance for a ring-shaped Ω), or for a finite union of such domains; we refer to [3,9] for a review of theoretical results and to [4,13,14,19,22] for a description of several numerical methods for these problems. In this configuration, one distinguishes the interior Bernoulli problem where the additional boundary condition similar to (1.4) is on the inner boundary, from the exterior Bernoulli problem where the additional boundary condition is on the outer boundary. The problem studied in this paper can be seen as a "limit" problem of the exterior boundary problem described in [16], since $\partial\Omega$ has one connected component and Ω is simply connected.

In comparison to the standard Bernoulli problems, $(\mathcal{F})$ presents several additional distinctive features, both from the theoretical and numerical point of view. The difficulties here stem from the particular geometric setting. Indeed, the constraint $\Omega \subset \mathbb{R}^N_+$ is such that the hyperplane $\{x_1 = 0\}$ behaves like an obstacle for the domain Ω and the free boundary $\partial\Omega \setminus K$. It is clear from the results in [24] that this constraint will be active as the optimal set $L^\star = (\partial\Omega^\star \setminus K) \cap \{x_1 = 0\}$ is not empty. This type of constraint is difficult to deal with in shape optimization and there has been very few attempts, if any, at solving these problems.

From the theoretical point of view, the difficulties are apparent in [24], but a proof technique used for the standard Bernoulli problem may be adapted to our particular setup. Indeed, a Beurling's technique and a Perron argument were used, in the same way as in [16–18].

https://doi.org/10.1051/cocv/2010049 Published online by Cambridge University Press

Nevertheless, the proof of the existence and uniqueness of the free boundary is mainly theoretical and no numerical algorithm may be deduced to construct Γ. From the numerical point of view, several problems arise that will be discussed in the next sections. The main issue is that Γ is a free boundary but the set $L = (\partial\Omega \setminus K) \cap \{x_1 = 0\}$ is a "free" set as well, in the sense that its length is unknown and should be obtained through the optimization process. In other words, the interface between L and Γ has to be determined and this creates a major difficulty for the numerical resolution.

The aim of this paper is twofold: on one hand we perform a detailed analysis of the geometrical properties of the free boundary Γ and in particular we are interested in the dependence of Γ on K. On the other hand, we introduce an efficient algorithm in order to compute a numerical approximation of Ω. In this way we perform a complete analysis of the problem.

First of all, using standard techniques for free boundary problems, we prove symmetry and monotonicity properties of the free boundary. These results are used further to prove the main theoretical result of the section in Section 3.3, where the asymptotic behavior of the free boundary, as the length of the subset K of the boundary diverges, is exhibited. The proof is based on a judicious cut-out of the optimal domain and on estimates of the solution of the associated partial differential equation to derive the variational formulation driving the solution of the "limit problem".

Secondly, we give a numerical algorithm for a numerical approximation of Ω. To determine the free boundary we use a shape optimization approach as in [13,14,19], where a penalization of one of the boundary condition in (1.1)–(1.4) using a shape functional is introduced. However, the original contribution of this paper regarding the numerical algorithm comes from the way how the "free" part L of the boundary is handled. Indeed, it has been proved in the theoretical study presented in [24] that the set $L = (\partial\Omega\setminus K) \cap \{x_1 = 0\}$ has nonzero length. The only equation satisfied on L is the Dirichlet condition, and a singularity naturally appears in the solution at the interface between K and L during the optimization process, due to the jump in boundary conditions. This singularity is a major issue for numerical algorithms: the usual numerical approaches for standard Bernoulli free boundary problems [13,14,19,20] cannot be used and a specific methodology has to be developed. A solution proposed in this paper consists in introducing a partial differential equation with special Robin boundary conditions depending on an asymptotically small parameter ε and approximating the solution of the free boundary problem. We then prove in Theorem 4.1 the convergence of the approximate solution to the solution of the free boundary problem, as ε goes to zero. In doing so we show the efficiency of a numerical algorithm that may be easily adapted to solve other problems where the free boundary meets a fixed boundary as well as free boundary problems with geometrical constraints or jumps in boundary conditions. Our implementation is based on a standard parameterization of the boundary using splines. Numerical results show the efficiency of the approach.

The paper is organized as follows. Section 2 is devoted to recalling basic concepts of shape sensitivity analysis. In Section 3, we provide qualitative properties of the free boundary Γ, precisely we exhibit symmetry and a monotonicity property with respect to the length of the set K as well as asymptotic properties of Γ. In Section 4, the shape optimization approach for the resolution of the free boundary problem and a penalization of the p.d.e. to handle the jump in boundary conditions are introduced. In Section 5, the shape derivative of the functionals are computed and used in the numerical simulations of $(\mathcal{F})$ in Sections 6 and 7.

2. Shape sensitivity analysis

To solve the free boundary problem $(\mathcal{F})$, we formulate it as a shape optimization problem, *i.e.* as the minimization of a functional which depends on the geometry of the domains $\Omega \subset \mathcal{O}$. In this way we may study the sensitivity with respect to perturbations of the shape and use it in a numerical algorithm. The shape sensitivity analysis is also useful to study the dependence of $\Omega^\star$ on the length of K, and in particular to derive the monotonicity of the domain $\Omega^\star$ with respect to the length of K.

The major difficulty in dealing with sets of shapes is that they do not have a vector space structure. In order to be able to define shape derivatives and study the sensitivity of shape functionals, we need to construct

https://doi.org/10.1051/cocv/2010049 Published online by Cambridge University Press

such a structure for the shape spaces. In the literature, this is done by considering perturbations of an initial domain; see [6,15,27].

Therefore, essentially two types of domain perturbations are considered in general. The first one is a *method of perturbation of the identity operator*, the second one, the *velocity* or *speed method* is based on the deformation obtained by the flow of a velocity field. The speed method is more general than the method of perturbation of the identity operator, and the equivalence between deformations obtained by a family of transformations and deformations obtained by the flow of velocity field may be shown [6,27]. The method of perturbation of the identity operator is a particular kind of domain transformation, and in this paper the main results will be given using a simplified speed method, but we point out that using one or the other is rather a matter of preference as several classical textbooks and authors rely on the method of perturbation of the identity operator as well.

For the presentation of the speed method, we mainly rely on the presentations in [6,27]. We also restrict ourselves to shape perturbations by *autonomous* vector fields, *i.e.* time-independent vector fields. Let $V : \mathbb{R}^N \to \mathbb{R}^N$ be an autonomous vector field. Assume that

$$V \in \mathcal{D}^k(\mathbb{R}^N, \mathbb{R}^N) = \{V \in \mathcal{C}^k(\mathbb{R}^N, \mathbb{R}^N),\ V \text{ has compact support}\}, \tag{2.1}$$

with $k \geq 0$.

For $\tau > 0$, we introduce a family of transformations $T_t(V)(X) = x(t, X)$ as the solution to the ordinary differential equation

$$\left\{ \begin{array}{rcl} \dfrac{\mathrm{d}}{\mathrm{d}t} x(t, X) & = & V(x(t, X)), \quad 0 < t < \tau, \\ x(0, X) & = & X \in \mathbb{R}^N. \end{array} \right. \tag{2.2}$$

For τ sufficiently small, the system (2.2) has a unique solution [27]. The mapping T_t allows to define a family of domains $\Omega_t = T_t(V)(\Omega)$ which may be used for the differentiation of the shape functional. We refer to [6], Chapter 7, and [27], Theorem 2.16, for theorems establishing the regularity of transformations T_t.

It is assumed that the shape functional $J(\Omega)$ is well-defined for any measurable set $\Omega \subset \mathbb{R}^N$. We introduce the following notions of differentiability with respect to the shape:

Definition 2.1 (Eulerian semiderivative)**.** Let $V \in \mathcal{D}^k(\mathbb{R}^N, \mathbb{R}^N)$ with $k \geq 0$, the *Eulerian semiderivative* of the shape functional $J(\Omega)$ at Ω in the direction V is defined as the limit

$$\mathrm{d}J(\Omega; V) = \lim_{t \searrow 0} \frac{J(\Omega_t) - J(\Omega)}{t}, \tag{2.3}$$

when the limit exists and is finite.

Definition 2.2 (shape differentiability)**.** The functional $J(\Omega)$ is *shape differentiable* (or *differentiable* for simplicity) at Ω if it has a Eulerian semiderivative at Ω in all directions V and the map

$$V \mapsto \mathrm{d}J(\Omega, V) \tag{2.4}$$

is linear and continuous from $\mathcal{D}^k(\mathbb{R}^N, \mathbb{R}^N)$ into $\mathbb{R}$. The map (2.4) is then sometimes denoted $\nabla J(\Omega)$ and referred to as the *shape gradient* of J and we have

$$\mathrm{d}J(\Omega, V) = \langle \nabla J(\Omega), V \rangle_{\mathcal{D}^{-k}(\mathbb{R}^N, \mathbb{R}^N), \mathcal{D}^k(\mathbb{R}^N, \mathbb{R}^N)}. \tag{2.5}$$

When the data is smooth enough, *i.e.* when the boundary of the domain Ω and the velocity field V are smooth enough (this will be specified later on), the shape derivative has a particular structure: it is concentrated on the boundary $\partial\Omega$ and depends only on the normal component of the velocity field V on the boundary $\partial\Omega$. This result, often called *structure theorem* or *Hadamard Formula*, is fundamental in shape optimization and will be observed in Theorem 5.1.

https://doi.org/10.1051/cocv/2010049 Published online by Cambridge University Press

3. Geometric properties and asymptotic behaviour

In shape optimization, once the existence and maybe uniqueness of an optimal domain have been obtained, an explicit representation of the domain, using a parameterization for instance usually cannot be achieved, except in some particular cases, for instance if the optimal domain has a simple shape such as a ball, ellipse or a regular polygon. On the other hand, it is usually possible to determine important geometric properties of the optimum, such as symmetry, connectivity, convexity for instance. In this section we show first of all that the optimal domain is symmetric with respect to the perpendicular bisector of the segment K, using a symmetrization argument. Then, we are interested in the asymptotic behaviour of the solution as the length of K goes to infinity. We are able to show that the optimal domain $\Omega^\star$ is monotonically increasing for the inclusion when the length of K increases, and that $\Omega^\star$ converges, in a sense that will be given in Theorem 3.2, to the infinite strip $(0,1)\times\mathbb{R}$.

The proofs presented in Sections 3.1 and 3.2 are quite standard and similar ideas of proofs may be found *e.g.* in [15–18].

3.1. Symmetry

In this subsection, we derive a symmetry property of the free boundary. The interest of such a remark is intrinsic and appears useful from a numerical point of view too, for instance to test the efficiency of the chosen algorithm.

In the two-dimensional case, we have the following result of symmetry:

Proposition 3.1. *Let $\Omega^\star$ be the solution of the free boundary problem (1.1)–(1.4). Assume, without loss of generality that (Ox_1) is the perpendicular bisector of K. Then, $\Omega^\star$ is symmetric with respect to (Ox_1).*

Proof. Like often, this proof is based on a symmetrization argument. It may be noticed that, according to the result stated in [24], Theorem 1, Ω is the unique solution of the overdetermined optimization problem

$$(\mathcal{B}_0):\left\{\begin{array}{ll}\text{minimize} & J(\Omega,u)\\ \text{subject to} & \Omega\in\mathcal{O},\ u\in H(\Omega),\end{array}\right.$$

where

$$H(\Omega)=\{u\in H^1(\Omega), u=1 \text{ on } K, u=0 \text{ on } \partial\Omega\backslash K \text{ and } |\nabla u|=1 \text{ on } \Gamma\},$$

and

$$J(\Omega,u)=\int_\Omega |\nabla u(x)|^2 \mathrm{d}x.$$

From now on, $\Omega^\star$ will denote the unique solution of $(\mathcal{B}_0)$, K being fixed. We denote by $\widehat{\Omega}$ the Steiner symmetrization of Ω with respect to the hyperplane $x_2=0$, *i.e.*

$$\widehat{\Omega}=\left\{x=(x',x_2) \text{ such that } -\frac{1}{2}|\Omega(x')|<x_2<\frac{1}{2}|\Omega(x')|,\ x'\in\Omega'\right\},$$

where

$$\Omega'=\{x'\in\mathbb{R} \text{ such that there exists } x_2 \text{ with } (x',x_2)\in\Omega^\star\}$$

and

$$\Omega(x')=\{x_2\in\mathbb{R} \text{ such that } (x',x_2)\in\Omega\},\ x'\in\Omega'.$$

By construction, $\widehat{\Omega}$ is symmetric with respect to the (Ox_1) axis. Let us also introduce $\widehat{u}$, defined by

$$\widehat{u}: x\in\widehat{\Omega}\mapsto \sup\{c \text{ such that } x\in\widehat{\omega^\star(c)}\},$$

https://doi.org/10.1051/cocv/2010049 Published online by Cambridge University Press

where $\omega^\star(c) = \{x \in \Omega^\star : u(x) \geq c\}$. Then, one may verify that $\widehat{u} \in H(\widehat{\Omega})$ and Polyà's inequality (see [15]) yields

$$J(\widehat{\Omega}, \widehat{u}) \leq J(\Omega^\star, u^\star).$$

Since $(\Omega^\star, u^\star)$ is a minimizer of J and using the uniqueness of the solution of $(\mathcal{B}_0)$, we get $\Omega^\star = \widehat{\Omega}$. □

Remark 3.1. This proof yields in addition that the direction of the normal vector at the intersection of Γ and (Ox_1) is (Ox_1).

3.2. Monotonicity

In this subsection, we show that $\Omega^\star$ is monotonically increasing for the inclusion when the length of K increases. For a given $a > 0$, define $K_a = \{0\} \times [-a, a]$. Let $(\mathcal{F}_a)$ denote problem $(\mathcal{F})$ with K_a instead of K and denote Ω_a and u_a the corresponding solutions. We have the following result on the monotonicity of Ω_a with respect to a.

Theorem 3.1. *Let $0 < a < b$, then $\Omega_a \subset \Omega_b$.*

Proof. According to [24], $(\mathcal{F}_a)$ has a solution for every $a > 0$ and $\partial\Omega_a$ is $C^{2+\alpha}$, $0 < \alpha < 1$. We argue by contradiction, assuming that $\Omega_a \not\subset \Omega_b$. Introduce, for $t \geq 1$, the set

$$\Omega_t = \{x \in \Omega_a : tx \in \Omega_a\}.$$

We also denote by $K_t := \{0\} \times [-ta, ta]$ and $\Gamma_t := \partial\Omega_t \backslash (\partial\Omega_t \cap (Ox_2))$. The domain Ω_t is obviously a convex set included in Ω_a for $t \geq 1$. Now denote

$$t_{\min} := \inf\{t \geq 1,\ \Omega_t \subset \Omega_b\}.$$

On one hand, $\Omega_a \subset \Omega_b$ is equivalent to $t_{\min} = 1$. On the other hand, if $\Omega_a \not\subset \Omega_b$, then $t_{\min} > 1$ and for t large enough, we clearly have $\Omega_t \subset \Omega_b$, therefore $t_{\min}$ is finite. In addition, if $\Omega_a \not\subset \Omega_b$ we have $\Gamma_{t_{\min}} \cap \Gamma_b \neq \emptyset$. Now, choose $y \in \Gamma_{t_{\min}} \cap \Gamma_b$. Let us introduce

$$u_{t_{\min}} : x \in \Omega_t \mapsto u_a(t_{\min} x).$$

Then, $u_{t_{\min}}$ verifies

$$\begin{aligned} -\Delta u_{t_{\min}} &= 0 \quad \text{in } \Omega_{t_{\min}}, \\ u_{t_{\min}} &= 1 \quad \text{on } K_{t_{\min}}, \\ u_{t_{\min}} &= 0 \quad \text{on } \Gamma_{t_{\min}}, \end{aligned}$$

so that, in view of $\Omega_{t_{\min}} \subset \Omega_b$ and $K_{t_{\min}} \subset K_b$, the maximum principle yields $u_b \geq u_{t_{\min}}$ in $\Omega_{t_{\min}}$. Consequently, the function $h = u_b - u_{t_{\min}}$ is harmonic in $\Omega_{t_{\min}}$, and since $h(y) = 0$, h reaches its lower bound at y. Applying Hopf's lemma (see [7]) thus yields $\partial_n h(y) < 0$ so that $|\nabla u_b(y)| \geq |\nabla u_{t_{\min}}(y)|$. Hence,

$$1 = |\nabla u_b(y)| \geq |\nabla u_{t_{\min}}(y)| = t_{\min} > 1,$$

which is absurd. Therefore we necessarily have $t_{\min} = 1$ and $\Omega_a \subset \Omega_b$. □

3.3. Asymptotic behaviour

We may now use the symmetry property of the free boundary to obtain the asymptotic properties of Ω_a when the length of K goes to infinity, *i.e.* we are interested in the behaviour of the free boundary Γ_a as $a \to \infty$.

https://doi.org/10.1051/cocv/2010049 Published online by Cambridge University Press

Let us say one word on our motivations for studying such a problem. First, this problem can be seen as a limit problem of the "unbounded case" studied in [18], Section 5, relative to the one phase free boundary problem for the p-Laplacian with non-constant Bernoulli boundary condition. Second, let us notice that the change of variable $x' = x/a$ and $y' = y/a$ transforms the free boundary (1.1)–(1.4) problem into

$$\begin{aligned} -\Delta z &= 0 \quad \text{in } \Omega, && (3.1)\\ z &= 1 \quad \text{on } K_1, && (3.2)\\ z &= 0 \quad \text{on } \partial\Omega \setminus K_1, && (3.3)\\ |\nabla z| &= a \quad \text{on } \Gamma = (\partial\Omega \setminus K_1) \cap \mathbb{R}^N_+, && (3.4) \end{aligned}$$

which proves that the solution of (3.1)–(3.4) is $h_{1/a}(\Omega_a)$, where $h_{1/a}$ denotes the homothety centered at the origin, with ratio $1/a$. Hence such a study permits also to study the role of the Lagrange multiplier associated with the volume constraint of the problem

$$\begin{cases} \min C(\Omega) \text{ where } C(\Omega) = \min\left\{\frac{1}{2}\int_\Omega |\nabla u_\Omega|^2,\ u = 1 \text{ on } K_1,\ u = 0 \text{ on } \partial\Omega\backslash K_1\right\} \\ \Omega \text{ quasi-open},\ |\Omega| = m, \end{cases}$$

since, as enlightened in [15], Chapter 6, the optimal domain is the solution of (3.1)–(3.4) for a certain constant $a > 0$. The study presented in this section permits to link the Lagrange multiplier to the constant m appearing in the volume constraint and to get some information on the limit case $a \to +\infty$.

We actually show that Γ_a converges, in an appropriate sense, to the line parallel to K_a and passing through the point $(1, 0)$. Let us introduce the infinite open strip

$$S =]0, 1[\times \mathbb{R},$$

and the open, bounded rectangle

$$R(b) =]0, 1[\times]-b, b[\subset S.$$

Let

$$u_S : x \in S \mapsto 1 - x_1.$$

Observe that, since Ω_a is solution of the free boundary problem (1.1)–(1.4), the curve $\Gamma_a \cap \{-a \le x_2 \le a\}$ is the graph of a concave $\mathcal{C}^{2,\alpha}$ function $x_2 \mapsto \psi_a(x_2)$ on $[-a, a]$. We have the following result:

Theorem 3.2. *The domain Ω_a converges to the strip S in the sense that for all $b > 0$, we have*

$$\psi_a \to 1, \ \textit{uniformly in } [-b, b], \ \textit{as } a \to +\infty. \tag{3.5}$$

We also have the convergence

$$u_a \to u_S \quad \textit{in } H^1(R(b)) \quad \textit{as } a \to \infty,$$

for the solution u_a of (1.1)–(1.4).

Proof. Let us introduce the function

$$v_a(x_1) = u_a(x_1, 0).$$

According to [15], Proposition 5.4.12, we have for a domain Ω of class $\mathcal{C}^2$ and $u : \overline{\Omega} \to \mathbb{R}$ of class $\mathcal{C}^2$

$$\Delta u = \Delta_\Gamma u + \mathcal{H}\partial_n u + \partial_n^2 u, \tag{3.6}$$

where $\Delta_\Gamma u$ denotes the Laplace-Beltrami operator. Applying formula (3.6) in the domains

$$\omega_a(c) := \{x \in \Omega_a,\ u_a(x) > c\},$$

https://doi.org/10.1051/cocv/2010049 Published online by Cambridge University Press

we get $\Delta_\Gamma u_a = 0$ on $\partial\omega_a(c)$, $\Delta u_a = 0$ due to (1.1) and thus

$$\partial_n^2 u_a = -\mathcal{H}_a \partial_n u_a \quad \text{on } \partial\omega_a(c), \tag{3.7}$$

where n is the outer unit normal vector to $\omega_a(c)$ and $\mathcal{H}_a(x)$ denotes here the curvature of $\partial\omega_a(c)$ at a point $x \in \partial\omega_a(c)$. Thanks to the symmetry of Ω_a with respect to the x_1-axis, we have $\partial_n u_a(x_1, 0) = v_a'(x_1)$ and $\partial_n^2 u_a(x_1, 0) = v_a''(x_1)$ for $x_1 \geq 0$. According to [24], the sets $\omega_a(c)$ are convex. Therefore $\mathcal{H}_a$ is positive on $\partial\omega_a(c)$ and $v_a(x_1)$ is non-increasing. Thus

$$v_a''(x_1) = -\mathcal{H}_a(x_1, 0) v_a'(x_1) \geq 0, \tag{3.8}$$

which means that v_a is convex. Let m_a be such that $\Gamma_a \cap (\mathbb{R} \times \{0\}) = (m_a, 0)$, *i.e.* the first coordinate of the intersection of the x_1-axis and the free boundary Γ_a. The function v_a satisfies

$$-v_a''(x_1) \leq 0 \quad \text{for } x_1 \in]0, m_a[, \tag{3.9}$$

$$v_a(0) = 1, \tag{3.10}$$

$$v_a(m_a) = 0, \tag{3.11}$$

$$v_a'(m_a) = -1. \tag{3.12}$$

In view of (3.9), v_a is convex on $[0, m_a]$. Since $v_a(0) = 1$ and $v_a(m_a) = 0$, then

$$v_a(x_1) \leq 1 - \frac{x_1}{m_a}.$$

Furthermore, $m_a \leq 1$, otherwise, due to the convexity of v_a, the Neumann condition (3.12) would not be satisfied. Since Ω_a is convex, this proves that $\Omega_a \subset S$ and that Ω_a is bounded.

Moreover, from Theorem 3.1, the map $a \mapsto \Omega_a$ is nondecreasing with respect to the inclusion. It follows that the sequence (m_a) is nondecreasing and bounded since $\Omega_a \subset S$. Hence, (m_a) converges to $m_\infty \leq 1$.

Let us define

$$u_\infty(x_1) = 1 - \frac{x_1}{m_\infty}.$$

The previous remarks ensure that for every $a > 0$, $v_a \leq u_\infty$.

Let $\mathcal{D}(a)$ be the line containing the points $(0, a)$ and $(\psi_a(b), b)$ and $\mathcal{T}(a)$ the line tangent to Γ_a at $(\psi_a(b), b)$. Let $s_\mathcal{D}(a)$ and $s_\mathcal{T}(a)$ denote the slopes of $\mathcal{D}(a)$ and $\mathcal{T}(a)$, respectively. For a fixed $b \in (0, a)$, we have

$$s_\mathcal{D}(a) = \frac{b - a}{\psi_a(b)} \to -\infty \quad \text{as } a \to \infty,$$

since $0 \leq \psi_a \leq 1$. Due to the convexity of Ω_a, we also have $s_\mathcal{T}(a) < s_\mathcal{D}(a)$. Therefore

$$s_\mathcal{T}(a) \to -\infty \quad \text{as } a \to \infty.$$

Thus, the slopes of the tangents to Γ_a go to infinity in $\Omega_a \cap R(b)$. Furthermore, due to the concavity of the function ψ_a, we get, by construction of $\mathcal{D}(a)$,

$$\frac{m_a}{a}(a - x_2) \leq \psi_a(x_2) \leq m_\infty, \ \forall a > 0, \ \forall x_2 \in [-b, b].$$

Hence, we obtain the pointwise convergence result:

$$\lim_{a \to +\infty} \psi_a(x_2) = m_\infty, \ \forall x_2 \in [-b, b], \tag{3.13}$$

which proves the uniform convergence of ψ_a to m_∞ as $a \to +\infty$.

https://doi.org/10.1051/cocv/2010049 Published online by Cambridge University Press

From now on, with a slight misuse of notation, u_a will also denote its extension by zero to all of S. Finally, let us prove the convergence

$$u_a \to u_\infty \quad \text{in } H^1(R_\infty(b)), \text{ as } a \to \infty,$$

where $R_\infty(b)$ denotes the rectangle whose edges are: $\Sigma_1 = \{0\}\times[-b,b]$, $\Sigma_2 = [0,m_\infty]\times\{b\}$, $\Sigma_3 = \{m_\infty\}\times[-b,b]$ and $\Sigma_4 = [0,m_\infty]\times\{-b\}$.

According to the zero Dirichlet conditions on Σ_3 and using Poincaré's inequality, proving the H^1-convergence is equivalent to show that

$$\int_{R_\infty(b)} |\nabla(u_a - u_\infty)|^2 \to 0 \quad \text{as } a \to \infty. \tag{3.14}$$

For our purposes, we introduce the curve $\widetilde{\Sigma}_2(a)$ described by the points $X_{a,b}$ solutions of the following ordinary differential equation

$$\begin{cases} \dfrac{\mathrm{d}X_{a,b}}{\mathrm{d}t}(t) = \nabla u_a(X_{a,b}(t)), \quad t>0, \\ X_{a,b}(0) = (0,b). \end{cases} \tag{3.15}$$

The curve $\widetilde{\Sigma}_2(a)$ is naturally extended along its tangent outside of Ω_a. $\widetilde{\Sigma}_2(a)$ can be seen as the curve originating at the point $(0,b)$ and perpendicular to the level set curves of Ω_a. We also introduce the curve $\widetilde{\Sigma}_4(a)$, symmetric to $\widetilde{\Sigma}_2(a)$ with respect to the x_1-axis. $\widetilde{\Sigma}_4(a)$ is obviously the set of points $Y_{a,b}$ solutions of the following ordinary differential equation

$$\begin{cases} \dfrac{\mathrm{d}Y_{a,b}}{\mathrm{d}t}(t) = \nabla u_a(Y_{a,b}(t)), \quad t>0, \\ Y_{a,b}(0) = (0,-b). \end{cases} \tag{3.16}$$

Then the set $Q_a(b)$ is defined as the region delimited by the x_2-axis on the left, the line parallel to the x_2-axis and passing through the point $(m_\infty,0)$ on the right and the curves $\widetilde{\Sigma}_2(a)$ and $\widetilde{\Sigma}_4(a)$ at the top and bottom. We also introduce the set $\widetilde{\Sigma}_3(a) := \overline{Q_a(b)} \cap (\{m_\infty\}\times\mathbb{R})$. See Figure 2 for a description of the sets $R_\infty(b)$ and $Q_a(b)$.

Since $R_\infty(b) \subset Q_a(b)$ (see Fig. 2), we have

$$\int_{R_\infty(b)} |\nabla(u_a - u_\infty)|^2 \le \int_{Q_a(b)} |\nabla(u_a - u_\infty)|^2.$$

Using Green's formula, we get

$$\begin{aligned} \int_{Q_a(b)} |\nabla(u_a - u_\infty)|^2 &= \int_{Q_a(b)\cap\Omega_a} |\nabla(u_a - u_\infty)|^2 + \int_{Q_a(b)\setminus\Omega_a} |\nabla(u_a - u_\infty)|^2 \\ &= -\int_{Q_a(b)\cap\Omega_a} (u_a - u_\infty)\Delta(u_a - u_\infty) - \int_{Q_a(b)\setminus\Omega_a} (u_a - u_\infty)\Delta(u_a - u_\infty) \\ &\quad + \int_{\partial Q_a(b)} (u_a - u_\infty)\partial_\nu(u_a - u_\infty) + \sum_{\pm} \int_{\Gamma_a\cap Q_a(b)} (u_a - u_\infty)\partial_{n^\pm}(u_a - u_\infty), \end{aligned}$$

where ν denotes the outer normal vector to $Q_a(b)$ on the boundary $\partial Q_a(b)$, n is the outer normal vector to Ω_a on the boundary Γ_a and $\partial_{n^\pm}$ is the normal derivative on Γ_a in the exterior or interior direction, the positive sign denoting the exterior direction to Ω_a. The functions u_a and u_∞ are harmonic, and using the various boundary conditions for u_a and u_∞ we get

$$\int_{Q_a(b)} |\nabla(u_a - u_\infty)|^2 = \int_{\widetilde{\Sigma}_2(a)\cup\widetilde{\Sigma}_4(a)} (u_a - u_\infty)\partial_\nu(u_a - u_\infty) + \int_{\Gamma_a\cap Q_a(b)} u_\infty.$$

https://doi.org/10.1051/cocv/2010049 Published online by Cambridge University Press

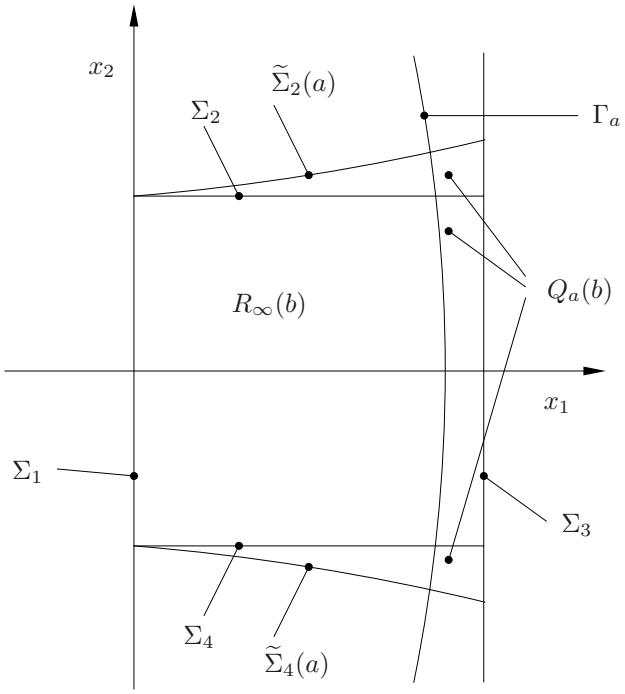


FIGURE 2. The sets $R_\infty(b)$ and $Q_a(b)$.

According to (3.13) and using $u_\infty = 0$ on Σ_3, we get

$$\int_{\Gamma_a \cap Q_a(b)} u_\infty = \int_{-b}^{b} u_\infty(\psi_a(x_2))\sqrt{1+\psi_a'(x_2)^2}\mathrm{d}x_2 \to 0 \quad \text{as } a \to \infty,$$

where we have also used the fact that $\psi_a'(x_2) \to 0$ for all $x_2 \in [-b, b]$. The limit function u_∞ depends only on x_1, thus we have $\partial_\nu u_\infty = 0$ on $\Sigma_2 \cup \Sigma_4$. Denote now $\widetilde{\psi}_a : [0, m_\infty] \to \mathbb{R}$ the graph of $\widetilde{\Sigma}_2(a)$ (which implies that $-\widetilde{\psi}_a$ is the graph of $\widetilde{\Sigma}_4(a)$). The slope of the tangents to the level sets of u_a converge to $-\infty$ as $a \to \infty$ in a similar way as for Γ_a, therefore $\partial_{x_2} u_a(x_1, \widetilde{\psi}_a(x_1))$ converges uniformly to 0 in $[0, m_\infty]$ as $a \to \infty$, and in view of (3.15) we have that $\widetilde{\psi}_a \to b$ uniformly in $[0, m_\infty]$ and since $(u_a - u_\infty)$ is uniformly bounded in Ω_a we have

$$\int_{\widetilde{\Sigma}_2(a) \cup \widetilde{\Sigma}_4(a)} (u_a - u_\infty)\partial_\nu u_\infty \to 0 \quad \text{as } a \to \infty. \tag{3.17}$$

In view of the definition of $Q_a(b)$, the outer normal vector ν to $Q_a(b)$ at a given point on $\widetilde{\Sigma}_2(a) \cup \widetilde{\Sigma}_4(a)$ is collinear with the tangent vector to the level set curve of Ω_a passing though the same point. Therefore $\partial_\nu u_a = 0$ on $\widetilde{\Sigma}_2(a) \cup \widetilde{\Sigma}_4(a)$ and we obtain finally

$$0 \leq \int_{R_\infty(b)} |\nabla(u_a - u_\infty)|^2 \leq \int_{Q_a(b)} |\nabla(u_a - u_\infty)|^2 \to 0 \quad \text{as } a \to \infty. \tag{3.18}$$

https://doi.org/10.1051/cocv/2010049 Published online by Cambridge University Press

The end of the proof consists in proving that $m_\infty = 1$. Let us introduce the test function φ as the solution of the partial differential equation

$$\begin{cases} -\Delta\varphi = 0 & \text{in } Q_a(b) \\ \varphi = 0 & \text{on } \Sigma_1 \cup \widetilde{\Sigma}_2(a) \cup \widetilde{\Sigma}_4(a) \\ \varphi = 1 & \text{on } \widetilde{\Sigma}_3(a). \end{cases} \tag{3.19}$$

It can be noticed that $\varphi \in H^1(R_\infty(b))$.

Using Green's formula and the same notations as previously, we get

$$\begin{aligned} \int_{Q_a(b)} \nabla(u_a - u_\infty)\cdot\nabla\varphi &= \int_{Q_a(b)\cap\Omega_a} \nabla(u_a - u_\infty)\cdot\nabla\varphi + \int_{Q_a(b)\setminus\Omega_a} \nabla(u_a - u_\infty)\cdot\nabla\varphi \\ &= -\int_{Q_a(b)\cap\Omega_a} \varphi\Delta(u_a - u_\infty) - \int_{Q_a(b)\setminus\Omega_a} \varphi\Delta(u_a - u_\infty) \\ &\quad + \int_{\partial Q_a(b)} \varphi\partial_\nu(u_a - u_\infty) + \sum_{\pm}\int_{\Gamma_a\cap Q_a(b)} \varphi\partial_{n^\pm}(u_a - u_\infty) \\ &= \int_{\widetilde{\Sigma}_2(a)\cup\widetilde{\Sigma}_4(a)} \varphi\partial_\nu(u_a - u_\infty) + \int_{\widetilde{\Sigma}_3(a)} \varphi\partial_n(u_a - u_\infty) - \int_{\Gamma_a\cap Q_a(b)} \varphi \\ &= \int_{\widetilde{\Sigma}_3(a)} \frac{\varphi}{m_\infty} - \int_{\Gamma_a\cap Q_a(b)} \varphi. \end{aligned}$$

According to (3.13), and since we deduce from (3.18) that

$$\int_{Q_a(b)} \nabla(u_a - u_\infty)\cdot\nabla\varphi \to 0 \quad \text{as } a \to \infty,$$

we get

$$\int_{\widetilde{\Sigma}_3(a)} \frac{\varphi}{m_\infty} - \int_{\widetilde{\Sigma}_3(a)} \varphi = 0,$$

which leads to

$$\left(\frac{1}{m_\infty} - 1\right) |\widetilde{\Sigma}_3(a)| = 0.$$

In other words, $m_\infty = 1$, which ends the proof. □

4. A penalization approach

4.1. **Shape optimization problems**

From now on we will assume that $N = 2$, *i.e.* we solve the problem in the plane. The problem for $N > 2$ may be treated with the same technique, but the numerical implementation becomes tedious. A classical approach to solve the free boundary problem is to penalize one of the boundary conditions in the over-determined system (1.1)–(1.4) within a shape optimization approach to find the free boundary. For instance one may consider the well-posed problem

$$-\Delta u_1 = 0 \quad \text{in } \Omega, \tag{4.1}$$

$$u_1 = 1 \quad \text{on } K, \tag{4.2}$$

$$u_1 = 0 \quad \text{on } \partial\Omega \setminus K, \tag{4.3}$$

https://doi.org/10.1051/cocv/2010049 Published online by Cambridge University Press

and enforce the second boundary condition (1.4) by solving the problem

$$(\mathcal{B}_1) : \left\{ \begin{array}{ll} \text{minimize} & J(\Omega) \\ \text{subject to} & \Omega \in \mathcal{O}, \end{array} \right. \tag{4.4}$$

with the functional J defined by

$$J(\Omega) = \int_\Gamma (\partial_n u_1 + 1)^2 \, \mathrm{d}\Gamma. \tag{4.5}$$

Indeed, using the maximum principle, one sees immediately that $u_1 \geq 0$ in Ω and since $u_1 = 0$ on $\partial\Omega \setminus K$, we obtain $\partial_n u_1 \leq 0$ on $\partial\Omega \setminus K$. Thus $|\nabla u_1| = -\partial_n u_1$ on $\partial\Omega \setminus K$ and the additional boundary condition (1.4) is equivalent to $\partial_n u_1 = -1$ on Γ. Hence, (4.5) corresponds to a penalization of condition (1.4). On one hand, if we denote $u_1^\star$ the unique solution of (1.1)–(1.4) associated to the optimal set $\Omega^\star$, we have

$$J(\Omega^\star) = 0,$$

so that the minimization problem (4.4) has a solution. On the other hand, if $J(\Omega^\star) = 0$, then $|\nabla u_1^\star| \equiv 1$ on Γ and therefore $u_1^\star$ is solution of (1.1)–(1.4). Thus $(\mathcal{F})$ and $(\mathcal{B}_1)$ are equivalent.

Another possibility is to penalize boundary condition (1.3) instead of (1.4) as in $(\mathcal{B}_1)$, in which case we consider the problem

$$-\Delta u_2 = 0 \quad \text{in } \Omega, \tag{4.6}$$

$$u_2 = 1 \quad \text{on } K, \tag{4.7}$$

$$u_2 = 0 \quad \text{on } L, \tag{4.8}$$

$$\partial_n u_2 = -1 \quad \text{on } \Gamma, \tag{4.9}$$

and the shape optimization problem is

$$(\mathcal{B}_2) : \left\{ \begin{array}{ll} \text{minimize} & J(\Omega) \\ \text{subject to} & \Omega \in \mathcal{O}, \end{array} \right. \tag{4.10}$$

with the functional J defined by

$$J(\Omega) = \int_\Gamma (u_2)^2 \, \mathrm{d}\Gamma. \tag{4.11}$$

Although the two approaches $(\mathcal{B}_1)$ and $(\mathcal{B}_2)$ are completely satisfying from a theoretical point of view, it is numerically easier to minimize a domain integral rather than a boundary integral as in (4.5) and (4.11). Therefore, a third classical approach is to solve

$$(\mathcal{B}_3) : \left\{ \begin{array}{ll} \text{minimize} & J(\Omega) \\ \text{subject to} & \Omega \in \mathcal{O}, \end{array} \right. \tag{4.12}$$

with the functional J defined by

$$J(\Omega) = \int_\Omega (u_1 - u_2)^2. \tag{4.13}$$

For the standard Bernoulli problems [3,9], solving $(\mathcal{B}_3)$ is an excellent approach as demonstrated in [13,14,19]. However, we are still not quite satisfied with it in our case. Indeed, it is well-known that due to the jump in boundary conditions at the interface between L and Γ in (4.8)–(4.9), the solution u_2 has a singular behaviour in the neighbourhood of this interface. To be more precise, let us define the points

$$\{A_1, A_2\} := \overline{L} \cap \overline{\Gamma},$$

https://doi.org/10.1051/cocv/2010049 Published online by Cambridge University Press

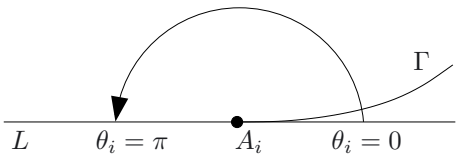


FIGURE 3. Polar coordinates with origin A_i, and such that $\theta_i = 0$ corresponds to the semi-axis tangent to Γ.

and the polar coordinates (r_i, θ_i) with origin the points A_i, $i = 1, 2$, and such that $\theta_i = 0$ corresponds to the semi-axis tangent to Γ; see Figure 3 for an illustration. Then, in the neighbourhood of A_i, u_2 has a singularity of the type

$$S_i(r_i, \theta_i) = c(A_i)\sqrt{r_i}\cos(\theta_i/2),$$

where $c(A_i)$ is the so-called *stress intensity factor* (see *e.g.* [12,21]).

These singularities are problematic for two reasons. The first difficulty is numerical: these singularities may produce inaccuracies when computing the solution near the points $\{A_1, A_2\}$, unless the proper numerical setting is used. It also possibly produces non-smooth deformations of the shape, which might create in turn undesired angles in the shape during the optimization procedure. The second difficulty is theoretical: since Γ is a free boundary with the constraint $\Omega \subset \mathbb{R}^N_+$, the points $\{A_1, A_2\}$ are also "free points", *i.e.* their optimal position is unknown in the same way as Γ is unknown. This means that the sensitivity with respect to those points has to be studied, which is doable but tedious, although interesting. The main ingredient in the computation of the shape sensitivity with respect to these points is the evaluation of the stress intensity factors $c(A_i)$.

4.2. **Penalization of the partial differential equation**

In order to deal with the aforementioned issue, we introduce a fourth approach, based on the penalization of the jump in the boundary conditions (4.8)–(4.9) for u_2. Let $\varepsilon \geq 0$ be a small real parameter, and let $\psi_\varepsilon \in \mathcal{C}(\mathbb{R}^+, \mathbb{R}^+)$ be a decreasing penalization function such that $\psi_\varepsilon \geq 0$, ψ_ε has compact support $[0, \beta_\varepsilon]$, and with the properties

$$\beta_\varepsilon \to 0 \text{ as } \varepsilon \to 0, \tag{4.14}$$

$$\psi_\varepsilon(0) \to \infty \text{ as } \varepsilon \to 0, \tag{4.15}$$

$$\psi_\varepsilon(x_1) \to 0 \text{ as } \varepsilon \to 0, \quad \forall x_1 > 0. \tag{4.16}$$

A simple example of such function is given by

$$\psi_\varepsilon(x_1) = \varepsilon^{-1}(\max(1 - \varepsilon^{-q}x_1, 0))^2 \mathbb{1}_{\mathbb{R}^+}, \tag{4.17}$$

with $q > 0$. Note that ψ_ε is decreasing, has compact support and verifies assumptions (4.14)–(4.16), with $\beta_\varepsilon = \varepsilon^q$. We will see in Proposition 4.1 that the choice of ψ_ε is conditioned by the shape of the domain. Then we consider the problem with Robin boundary conditions

$$-\Delta u_{2,\varepsilon} = 0 \quad \text{in } \Omega, \tag{4.18}$$

$$u_{2,\varepsilon} = 1 \quad \text{on } K, \tag{4.19}$$

$$\partial_n u_{2,\varepsilon} + \psi_\varepsilon(x_1) u_{2,\varepsilon} = -1 \quad \text{on } \partial\Omega \setminus K. \tag{4.20}$$

The function $u_{2,\varepsilon}$ is a penalization of u_2 in the sense that $u_{2,\varepsilon} \to u_2$ as $\varepsilon \to 0$ in $H^1(\Omega)$ if ψ_ε is properly chosen. The following proposition ensures the H^1-convergence of $u_{2,\varepsilon}$ to the desired function. It may be noticed that an explicit choice of function ψ_ε providing the convergence is given in the statement of this proposition.

https://doi.org/10.1051/cocv/2010049 Published online by Cambridge University Press

Proposition 4.1. *Let Ω be an open bounded domain. Then for ψ_ε given by (4.17), there exists a unique solution to (4.18)–(4.20) which satisfies*

$$u_{2,\varepsilon} \to u_2 \quad \text{in } H^1(\Omega) \quad \text{as } \varepsilon \to 0. \tag{4.21}$$

Proof. In the sequel, c will denote a generic positive constant which may change its value throughout the proof and does not depend on the parameter ε.

We shall prove that the difference

$$v_\varepsilon = u_2 - u_{2,\varepsilon}$$

converges to zero in $H^1(\Omega)$. The remainder v_ε satisfies, according to (4.6)–(4.9) and (4.18)–(4.20)

$$-\Delta v_\varepsilon = 0 \quad \text{in } \Omega, \tag{4.22}$$
$$v_\varepsilon = 0 \quad \text{on } K, \tag{4.23}$$
$$\partial_n v_\varepsilon + \psi_\varepsilon(0) v_\varepsilon = 1 + \partial_n u_2 \quad \text{on } L, \tag{4.24}$$
$$\partial_n v_\varepsilon + \psi_\varepsilon(x_1) v_\varepsilon = \psi_\varepsilon(x_1) u_2 \quad \text{on } \Gamma. \tag{4.25}$$

Multiplying by v_ε on both sides of (4.22), integrating on Ω and using Green's formula, we end up with

$$\int_\Omega |\nabla v_\varepsilon|^2 + \int_{\partial\Omega} (v_\varepsilon)^2 \psi_\varepsilon = \int_\Gamma \psi_\varepsilon u_2 v_\varepsilon + \int_L (1 + \partial_n u_2) v_\varepsilon. \tag{4.26}$$

Since $v_\varepsilon = 0$ on K we may apply Poincaré's theorem and (4.26) implies

$$\nu \|v_\varepsilon\|^2_{H^1(\Omega)} \le c \left(\|\psi_\varepsilon u_2\|_{L^2(\Gamma)} \|v_\varepsilon\|_{L^2(\Gamma)} + \|1 + \partial_n u_2\|_{L^2(L)} \|v_\varepsilon\|_{L^2(L)} \right). \tag{4.27}$$

According to the trace theorem and Sobolev's imbedding theorem, we have

$$\|v_\varepsilon\|_{L^2(\Gamma)} \le c \|v_\varepsilon\|_{H^{1/2}(\Gamma)} \le c \|v_\varepsilon\|_{H^1(\Omega)},$$
$$\|v_\varepsilon\|_{L^2(L)} \le c \|v_\varepsilon\|_{H^{1/2}(L)} \le c \|v_\varepsilon\|_{H^1(\Omega)}.$$

Hence, according to (4.27), we get

$$\|v_\varepsilon\|_{H^1(\Omega)} \le c \|\psi_\varepsilon u_2\|_{L^2(\Gamma)} + c \|1 + \partial_n u_2\|_{L^2(L)}. \tag{4.28}$$

Now we prove that $\|\psi_\varepsilon u_2\|_{L^2(\Gamma)} \to 0$ as $\varepsilon \to 0$. We may assume that the system of Cartesian coordinates (O, x_1, x_2) is such that the origin O is one of the points A_1 or A_2 and that Γ is locally above the x_1-axis; see Figure 4. Since Ω is convex, there exist $\delta > 0$ and two constants $\alpha > 0$ and β such that for all $x_1 \in (0, \delta)$, Γ is the graph of a convex function f of x_1. For our choice of ψ_ε, since supp $\psi_\varepsilon = [0, \beta_\varepsilon]$, we have the estimate

$$\begin{aligned} \|\psi_\varepsilon u_2\|^2_{L^2(\Gamma)} &= \int_\Gamma (\psi_\varepsilon u_2)^2 \\ &\le \psi_\varepsilon(0)^2 \int_0^{\beta_\varepsilon} (u_2)^2 \sqrt{1 + f'(x_1)^2}\, \mathrm{d}x_1. \end{aligned}$$

According to [12,21] and our previous remarks in Section 4.1, we have $u_2 = \sqrt{r}\cos(\theta/2) + u_\infty$, with $u_\infty \in H^2(\Omega)$, and (r, θ) are the polar coordinates defined previously with origin 0. Thus there exists a constant c such that

$$|u_2| \le c\sqrt{r}\cos(\theta/2)$$

https://doi.org/10.1051/cocv/2010049 Published online by Cambridge University Press

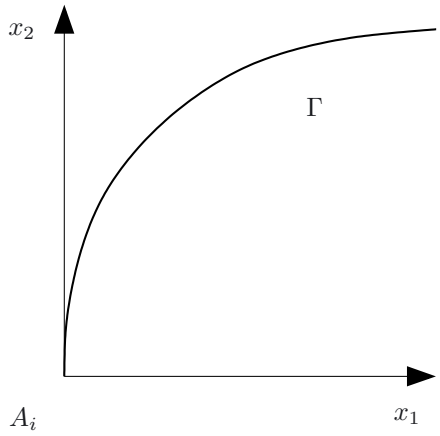


FIGURE 4. Γ is locally the graph of a convex function, with a tangent to the x_2-axis.

in a neighborhood of 0 with $\theta \in (0, \pi/2)$. Indeed, u_∞ is H^2 therefore C^1 in a neighborhood of 0 and then has an expansion of the form: $u_\infty = c_s r + o(r)$, as $r \to 0$. Note that $r = \sqrt{x_1^2 + x_2^2}$ and thus $r = \sqrt{x_1^2 + f(x_1)^2}$ on Γ. Then

$$\begin{aligned}\|\psi_\varepsilon u_2\|_{L^2(\Gamma)} &\le c\psi_\varepsilon(0) \left(\int_0^{\beta_\varepsilon} (\sqrt{r}\cos(\theta/2))^2 \sqrt{1 + f'(x_1)^2}\, \mathrm{d}x_1 \right)^{1/2} \\ &\le c\psi_\varepsilon(0) \left(\int_0^{\beta_\varepsilon} \sqrt{(x_1^2 + f(x_1)^2)(1 + f'(x_1)^2)}\, \mathrm{d}x_1 \right)^{1/2}.\end{aligned}$$

The function f is convex and $f(0) = 0$, thus $f' > 0$ for ε small enough. Since the boundary Γ is tangent to the (Ox_2) axis, we have

$$\begin{aligned} f'(x_1) &\to \infty \quad \text{as } x_1 \to 0^+, \\ x_1 &= o(f(x_1)) \quad \text{as } x_1 \to 0^+. \end{aligned}$$

Thus, for $\varepsilon > 0$ small enough

$$\begin{aligned}\|\psi_\varepsilon u_2\|_{L^2(\Gamma)} &\le c\psi_\varepsilon(0) \left(\int_0^{\beta_\varepsilon} f(x_1) f'(x_1)\, \mathrm{d}x_1 \right)^{1/2} \\ &\le c\psi_\varepsilon(0) \left(f(\beta_\varepsilon)^2 \right)^{1/2} = c\psi_\varepsilon(0) f(\beta_\varepsilon).\end{aligned}$$

Since $f(x_1) \to 0$ as $x_1 \to 0$, we may choose $\psi_\varepsilon(0)$ and β_ε in order to obtain $\psi_\varepsilon(0) f(\beta_\varepsilon) \to 0$ as $\varepsilon \to 0$ and

$$\|\psi_\varepsilon u_2\|_{L^2(\Gamma)} \to 0 \quad \text{as } \varepsilon \to 0. \tag{4.29}$$

Then, in view of (4.28), we may deduce that $\|v_\varepsilon\|_{H^1(\Omega)}$ is bounded for the appropriate choice of ψ_ε. Consequently, $\|v_\varepsilon\|_{L^2(\Gamma)}$ and $\|v_\varepsilon\|_{L^2(L)}$ are also bounded. Using (4.26), we may also write

$$\begin{aligned}\psi_\varepsilon(0)\|v_\varepsilon\|_{L^2(L)}^2 &= \int_L (v_\varepsilon)^2 \psi_\varepsilon \le \int_{\partial\Omega} (v_\varepsilon)^2 \psi_\varepsilon \\ &\le \|\psi_\varepsilon u_2\|_{L^2(\Gamma)} \|v_\varepsilon\|_{L^2(\Gamma)} + \|1 + \partial_n u_2\|_{L^2(L)} \|v_\varepsilon\|_{L^2(L)}. \end{aligned} \tag{4.30}$$

https://doi.org/10.1051/cocv/2010049 Published online by Cambridge University Press

Since $\psi_\varepsilon(0) \to \infty$ as $\varepsilon \to 0$ and all terms in (4.30) are bounded, we necessarily have

$$\|v_\varepsilon\|_{L^2(L)} \to 0 \text{ as } \varepsilon \to 0.$$

Finally going back to (4.27) and using the previous results, we obtain

$$\|v_\varepsilon\|_{H^1(\Omega)} \to 0 \text{ as } \varepsilon \to 0,$$

and this proves $u_{2,\varepsilon} \to u_2$ as $\varepsilon \to 0$, in $H^1(\Omega)$. □

The following theorem gives a mathematical justification of the numerical scheme implemented in Section 6 to find the solution of the free Bernoulli problem $(\mathcal{F})$, based on the use of a penalized functional J_ε defined by

$$J_\varepsilon(\Omega) = \int_\Omega (u_{2,\varepsilon} - u_1)^2, \tag{4.31}$$

where u_1 is the solution of (4.1)–(4.3) and $u_{2,\varepsilon}$ is the solution of (4.18)–(4.20).

Theorem 4.1. *One has*

$$\lim_{\varepsilon \to 0} \inf_{\Omega \in \mathcal{O}} (J_\varepsilon(\Omega) - J(\Omega)) = 0.$$

Proof. The main ingredient of this proof is the result stated in Proposition 4.1. Indeed, this proposition yields in particular the convergence of $u_{2,\varepsilon}$ to u_2 in $L^2(\Omega)$, when Ω is a fixed element of $\mathcal{O}$. It follows immediately that

$$J_\varepsilon(\Omega) \to J(\Omega), \text{ as } \varepsilon \to 0.$$

Let us denote by $\Omega^\star$ the solution of the free Bernoulli problem $(\mathcal{F})$. Then, we obviously have

$$\inf_{\Omega \in \mathcal{O}} J_\varepsilon(\Omega) \leq J_\varepsilon(\Omega^\star).$$

Then, going to the limit as $\varepsilon \to 0$ yields

$$0 \leq \lim_{\varepsilon \to 0} \inf_{\Omega \in \mathcal{O}} J_\varepsilon(\Omega) \leq \lim_{\varepsilon \to 0} J_\varepsilon(\Omega^\star) = J(\Omega^\star) = 0.$$ □

Remark 4.1. Theorem 4.1 does not imply the existence of solutions for the problem $\inf\{J_\varepsilon(\Omega),\ \Omega \in \mathcal{O}\}$ and the following questions remain open: (i) existence of a minimizer $\Omega_\varepsilon^\star$ for this problem, (ii) compactness of $(\Omega_\varepsilon^\star)$ for an appropriate topology of domains. These problems appear difficult since to solve it, we probably need to establish a Sverak-like theorem for the Laplacian with Robin boundary conditions and some counter examples (see *e.g.* [5]) suggest that this is in general not true.

Nevertheless, if (i) and (ii) are true, Theorem 4.1 implies the convergence as $\varepsilon \to 0$, of $\Omega_\varepsilon^\star$ to $\Omega^\star$, the solution of (1.1)–(1.4).

5. Shape derivative for the penalized Bernoulli problem

In order to stay in the class of domains $\mathcal{O}$, the speed V should satisfy

$$V(x) = 0 \quad \forall x \in K, \tag{5.1}$$

$$V(x) \cdot n(x) < 0 \quad \forall x \in L. \tag{5.2}$$

Condition (5.1) will be taken into account in the algorithm, and (5.2) will be guaranteed by our optimization algorithm. We have the following result for the shape derivative $\mathrm{d}J_\varepsilon(\Omega; V)$ of $J_\varepsilon(\Omega)$:

https://doi.org/10.1051/cocv/2010049 Published online by Cambridge University Press

Theorem 5.1. *The shape derivative* $\mathrm{d}J_\varepsilon(\Omega;V)$ *of* J_ε *at* Ω *in the direction* V *is given by*

$$\begin{aligned}\mathrm{d}J_\varepsilon(\Omega;V) &= \int_\Gamma \left(\nabla p_1\cdot\nabla u_1+\nabla p_2\cdot\nabla u_{2,\varepsilon}+p_2\mathcal{H}+(u_1-u_{2,\varepsilon})^2\right)V\cdot n\,\mathrm{d}\Gamma,\\ &\quad+\int_L(\nabla p_1\cdot\nabla u_1-\nabla p_2\cdot\nabla u_{2,\varepsilon})\,V\cdot n\,\mathrm{d}L,\end{aligned}$$

where $\mathcal{H}$ *is the mean curvature of* Γ *and* p_1, p_2 *are given by* (5.12)–(5.13) *and* (5.14)–(5.16), *respectively.*

Proof. According to [6,15,27], the shape derivative of J_ε is given by

$$\mathrm{d}J_\varepsilon(\Omega;V)=\int_\Omega 2(u_1-u_2)(u_1'-u_{2,\varepsilon}')+\int_{\partial\Omega}(u_1-u_{2,\varepsilon})^2V\cdot n, \tag{5.3}$$

where u_1' and $u_{2,\varepsilon}'$ are the so-called *shape derivatives* of u_1 and u_2, respectively, and solve

$$\begin{aligned}-\Delta u_1' &= 0 \quad \text{in } \Omega, &(5.4)\\ u_1' &= 0 \quad \text{on } K, &(5.5)\\ u_1' &= -\partial_n u_1 V\cdot n \quad \text{on } \partial\Omega\setminus K, &(5.6)\\ -\Delta u_{2,\varepsilon}' &= 0 \quad \text{in } \Omega, &(5.7)\\ u_{2,\varepsilon}' &= 0 \quad \text{on } K, &(5.8)\\ u_{2,\varepsilon}' &= -\partial_n u_{2,\varepsilon} V\cdot n \quad \text{on } L, &(5.9)\\ \partial_n u_{2,\varepsilon}'+\psi_\varepsilon u_{2,\varepsilon}' &= \mathrm{div}_\Gamma(V\cdot n\nabla_\Gamma u_{2,\varepsilon})-\mathcal{H}V\cdot n-\psi_\varepsilon\partial_n u_{2,\varepsilon}V\cdot n \quad \text{on } \Gamma, &(5.10)\end{aligned}$$

where $\mathcal{H}$ denotes the mean curvature of Γ, and ∇_Γ is the tangential gradient on Γ defined by

$$\nabla_\Gamma u=\nabla u-(\partial_n u)n.$$

Note that u_1' and $u_{2,\varepsilon}'$ both vanish on K, indeed, K is fixed due to (5.1) which follows from the definition of our problem and of the class $\mathcal{O}$. Further we will also need

$$\partial_n u_{2,\varepsilon}'=\mathrm{div}_\Gamma(V\cdot n\nabla_\Gamma u_{2,\varepsilon})-\mathcal{H}V\cdot n \quad \text{on } \Gamma, \tag{5.11}$$

which is obtained in the same way as (5.10). We introduce the adjoint states p_1 and p_2

$$\begin{aligned}-\Delta p_1 &= 2(u_1-u_{2,\varepsilon}) \quad \text{in } \Omega, &(5.12)\\ p_1 &= 0 \quad \text{on } \partial\Omega, &(5.13)\\ -\Delta p_2 &= 2(u_1-u_{2,\varepsilon}) \quad \text{in } \Omega, &(5.14)\\ p_2 &= 0 \quad \text{on } L\cup K, &(5.15)\\ \partial_n p_2 &= 0 \quad \text{on } \Gamma. &(5.16)\end{aligned}$$

https://doi.org/10.1051/cocv/2010049 Published online by Cambridge University Press

Note that p_1 and p_2 actually depend on ε although this is not apparent in the notation for the sake of readability. Using the adjoint states, we are able to compute

$$\begin{aligned}\int_\Omega 2(u_1-u_{2,\varepsilon})u_1' &= \int_\Omega -\Delta p_1 u_1' \\ &= \int_\Omega -\Delta u_1' p_1 - \int_{\partial\Omega} \partial_n p_1 u_1' - p_1\partial_n u_1 \\ &= -\int_{\partial\Omega\setminus K} \partial_n p_1 u_1' \\ &= \int_{\partial\Omega\setminus K} \partial_n p_1 \partial_n u_1 V\cdot n.\end{aligned}$$

Observing that $\nabla p_1 = \partial_n p_1 n$ and $\nabla u_1 = \partial_n u_1 n$ on $\partial\Omega\setminus K$ due to (4.3) and (5.13) we obtain

$$\int_\Omega 2(u_1-u_{2,\varepsilon})u_1' \mathrm{d}x = \int_{\partial\Omega\setminus K} \nabla p_1\cdot\nabla u_1 V\cdot n. \tag{5.17}$$

For the other domain integral in (5.3) we get

$$\begin{aligned}\int_\Omega 2(u_1-u_{2,\varepsilon})u_{2,\varepsilon}' &= \int_\Omega -\Delta p_2 u_{2,\varepsilon}' \\ &= \int_\Omega -\Delta u_{2,\varepsilon}' p_2 - \int_{\partial\Omega}(\partial_n p_2 u_{2,\varepsilon}' - p_2\partial_n u_{2,\varepsilon}').\end{aligned}$$

At this point we make use of (5.7)–(5.11) and we get

$$\int_\Omega 2(u_1-u_{2,\varepsilon})u_{2,\varepsilon}' = \int_\Gamma p_2(\mathrm{div}_\Gamma(V\cdot n\nabla_\Gamma u_{2,\varepsilon}) - \mathcal{H}V\cdot n)\mathrm{d}\Gamma + \int_L \partial_n p_2\partial_n u_{2,\varepsilon} V\cdot n\ \mathrm{d}L.$$

Applying classical tangential calculus to the above equation (see [27], Prop. 2.57, for instance) we have

$$\begin{aligned}\int_\Omega 2(u_1-u_{2,\varepsilon})u_{2,\varepsilon}' &= -\int_\Gamma(\nabla_\Gamma p_2\cdot\nabla_\Gamma u_{2,\varepsilon} V\cdot n - p_2\mathcal{H}V\cdot n)\mathrm{d}\Gamma + \int_L \partial_n p_2\partial_n u_{2,\varepsilon}V\cdot n\ \mathrm{d}L \\ &= -\int_\Gamma(\nabla p_2\cdot\nabla u_{2,\varepsilon} V\cdot n - p_2\mathcal{H}V\cdot n)\mathrm{d}\Gamma + \int_L \nabla p_2\cdot\nabla u_{2,\varepsilon}V\cdot n\ \mathrm{d}L,\end{aligned}$$

and the proof is complete. □

6. Numerical scheme

6.1. **Parameterization** *versus* **level set method**

For the numerical realization of shape optimization problems, the main issue is the representation of the moving shape Ω. Several different techniques are available: for our purpose, the most appropriate methods would be *parameterization* and the *level set method*. In the parameterization method for two-dimensional problems, curves are typically represented as splines given by control points $\xi_k = (\xi_{1,k}, \xi_{2,k})$, $k = 0, ..., m$ with $m \in \mathbb{N}^*$. The coordinates of these control points then become the shape design variables. In the level set method, the boundary of the domain in $\mathbb{R}^N$ is implicitly given by the zero level set of a function in $\mathbb{R}^{N+1}$. Parameterization methods are the easiest to implement if the topology of the domain Ω does not change

https://doi.org/10.1051/cocv/2010049 Published online by Cambridge University Press

in the course of iterations, whereas the level set method is more technical to implement but thanks to the implicit representation, it allows to handle easily topological changes of the domain, such as the creation of holes or the merging of two connected components.

For instance, in [4,22], the level set method is used to solve Bernoulli free boundary problem where the number of connected components is not known beforehand. In our case, we are solving the free boundary problem $(\mathcal{F})$ in the class $\mathcal{O}$ of convex domains, thus the domains only have one connected component and the topology is known. In this case it is better to opt for the parameterization method which is easier to implement and lighter in terms of computations.

The free boundary $\Gamma \subsetneq \partial\Omega$ is represented with the help of a Bezier curve of degree $m \in \mathbb{N}^*$. Let

$$x(s) = (x_1(s), x_2(s)), \quad s \in [0,1]$$

be a parametric representation of the open curve Γ and let

$$\xi_k = (\xi_{1,k}, \xi_{2,k}), \quad k = 0, \dots, m$$

be a set of $m+1$ control points such that the parameterization of Γ satisfies

$$x(s) = (x_1(s), x_2(s)) = \sum_{k=0}^{m} B_{k,m}(s)\xi_k, \tag{6.1}$$

where

$$B_{k,m}(s) = \binom{m}{k} s^k (1-s)^{m-k}, \tag{6.2}$$

and $\binom{m}{k}$ are the binomial coefficients. The geometric features such as the unit tangent $\tau(s)$, unit normal $n(s)$ and curvature $\mathcal{H}(s)$ are easily obtained from the representation (6.1). Indeed we have

$$\tau(s) = x'(s)/|x'(s)|, \tag{6.3}$$

with

$$x'(s) = \sum_{k=0}^{m} B'_{k,m}(s)\xi_k. \tag{6.4}$$

The coefficients $B'_{k,m}(s)$ are derived from (6.2)

$$B'_{k,m}(s) = \binom{m}{k} \left[k s^{k-1}(1-s)^{m-k} \mathbb{1}_{\{k \geq 1\}} + (k-m) s^k (1-s)^{m-k-1} \mathbb{1}_{\{k \leq m-1\}} \right]. \tag{6.5}$$

Since $n(s) \cdot \tau(s) = 0$, we deduce the expression for the unit normal $n(s)$

$$n(s) = \frac{\sum_{k=0}^{m} B'_{k,m}(s)\xi_k^{\perp}}{\left| \sum_{k=0}^{m} B'_{k,m}(s)\xi_k^{\perp} \right|}, \tag{6.6}$$

with $\xi_k^{\perp} := (\xi_{2,k}, -\xi_{1,k})$. The curvature $\mathcal{H}(s)$ is obtained with the help of formula

$$\tau'(s) = \mathcal{H}(s) n(s). \tag{6.7}$$

Thus we take

$$\mathcal{H}(s) = \tau'(s) \cdot n(s). \tag{6.8}$$

https://doi.org/10.1051/cocv/2010049 Published online by Cambridge University Press

Remark 6.1. According to (6.3), (6.4) and (6.5), we obtain

$$\tau(0) = \frac{\xi_1 - \xi_0}{|\xi_1 - \xi_0|}, \quad \tau(1) = \frac{\xi_m - \xi_{m-1}}{|\xi_m - \xi_{m-1}|}. \tag{6.9}$$

Thus, in order to create a curve which is tangent to the axis $\{x_1 = 0\}$, we need to take ξ_0, ξ_1 and ξ_{m-1}, ξ_m on $\{x_1 = 0\}$.

6.2. **Algorithm**

For the numerical algorithm we use a gradient projection method in order to deal with the geometric constraint $\Omega \subset \mathbb{R}^N_+$; see the textbooks [20,25] for details on the method. A solution for dealing with the shape optimization problems with a convexity constraint is to parameterize the boundary using a support function w. If one uses a polar coordinates representation (r, θ) for the domains, namely

$$\Omega_w := \left\{ (r, \theta) \in [0, \infty) \times \mathbb{R};\ r < \frac{1}{w(\theta)} \right\},$$

where w is a positive and 2π-periodic function, then Ω_w is convex if and only if $w'' + w \geq 0$; see [23] for details. However, in our case, the convexity constraint for Ω is not implemented (*i.e.* we relax this constraint) for the sake of simplicity, but the convexity property is observed at every iteration and in particular for the optimal domain if the initial domain is convex. Moreover, Theorem 6.6.2 of [15] may be easily generalized in our case and guarantees the convexity of the solution of the free boundary problem $(\mathcal{F})$ even if the convexity hypothesis were not contained in the set $\mathcal{O}$.

We will denote by a superscript (l) an object at iteration l. The algorithm is as follows: we are looking for an update of the design variable ξ_k of the type

$$\xi_k^{(l+1)} = P(\xi_k^{(l)} + \alpha \mathrm{d}\xi_k^{(l)}), \tag{6.10}$$

where P stands for the projection on the set of constraints and α is the steplength which has to be determined by an appropriate linesearch. In our case, the constraint is $\Omega \subset \mathbb{R}^N_+$, which implies the constraint

$$x_1(s) \geq 0, \quad \forall s \in [0, 1]. \tag{6.11}$$

In view of (6.1), it is difficult to directly interpret the constraint (6.11) for individual control points ξ_k. We choose therefore to impose the stronger constraint

$$\xi_{1,k} \geq 0, \quad \forall k \in \{1, \dots, m\} \tag{6.12}$$

for the control points. Constraint (6.12) is stronger than (6.11), indeed, on one hand there might exist a ξ_k such that $\xi_{1,k} < 0$ while (6.11) is still satisfied, but on the other hand, condition (6.12) implies (6.11). However, in our case, the tips $x(0)$ and $x(1)$ of Γ are moving and the constraint should not be active for the points of Γ on the optimal domain. With (6.12) we only guarantee that the domain stays feasible, *i.e.* $\Omega \in \mathbb{R}^N_+$ for all iterates. In view of Remark 6.1, we also impose

$$\xi_{2,0} = \xi_{2,1} = \xi_{2,m-1} = \xi_{2,m} = 0$$

https://doi.org/10.1051/cocv/2010049 Published online by Cambridge University Press

in order to preserve the tangent to the axis $\{x_1 = 0\}$ at the tips of Γ. Therefore, for $k = 0, ..., m$, $\xi_k^{(l)}$ is updated using,

$$\xi_{1,k}^{(l+1)} = \max\left(\xi_{1,k}^{(l)} + \alpha \mathrm{d}\xi_{1,k}^{(l)}, 0\right), \tag{6.13}$$

$$\xi_{2,k}^{(l+1)} = \xi_{2,k}^{(l)} + \alpha \mathrm{d}\xi_{2,k}^{(l)}, \tag{6.14}$$

$$\mathrm{d}\xi_{2,0}^{(l)} = \mathrm{d}\xi_{2,1}^{(l)} = 0, \tag{6.15}$$

$$\mathrm{d}\xi_{2,m-1}^{(l)} = \mathrm{d}\xi_{2,m}^{(l)} = 0. \tag{6.16}$$

The link between the perturbation field V and the step $\mathrm{d}\xi_k$ is directly established using (6.1), and we obtain

$$V(x(s)) = \sum_{k=0}^{m} B_{k,m}(s)\mathrm{d}\xi_k. \tag{6.17}$$

Thus, with a shape derivative given by

$$\mathrm{d}J_\varepsilon(\Omega; V) = \int_{\partial\Omega} \nabla J_\varepsilon(x) V(x) \cdot n(x)\, \mathrm{d}\Gamma(x) \tag{6.18}$$

as in Theorem 5.1, we obtain using (6.17) and (6.18)

$$\begin{aligned}
\mathrm{d}J_\varepsilon(\Omega; V) &= \int_0^1 \nabla J_\varepsilon(x(s)) V(x(s)) \cdot n(s) |x'(s)|\, \mathrm{d}s \\
&= \int_0^1 \nabla J_\varepsilon(x(s)) \left[\sum_{k=0}^{m} B_{k,m}(s)\mathrm{d}\xi_k\right] \cdot n(s)|x'(s)|\, \mathrm{d}s \\
&= \sum_{k=0}^{m} \mathrm{d}\xi_k \cdot \int_0^1 \nabla J_\varepsilon(x(s)) B_{k,m}(s) n(s) |x'(s)|\, \mathrm{d}s.
\end{aligned}$$

Thus, a descent direction for the algorithm is given by

$$\mathrm{d}\xi_k = -\int_0^1 \nabla J_\varepsilon(x(s)) B_{k,m}(s) n(s) |x'(s)|\, \mathrm{d}s, \tag{6.19}$$

and the update is then performed according to (6.13)–(6.16). The step α is determined by a line search in the spirit of the gradient projection algorithm [20]: a step is validated if we observe a sufficient decrease of the shape functional J_ε measured by

$$J_\varepsilon(\Omega^{(l+1)}) - J_\varepsilon(\Omega^{(l)}) \leq -\frac{\alpha}{\lambda} \sum_{k=1}^{m} \left|\xi_k^{(l+1)} - \xi_k^{(l)}\right|^2,$$

where $|\cdot|$ denotes the Euclidean distance. The line search consists in finding the smallest integer a (the smallest possible being $a = 0$) such that

$$\alpha = \mu\eta^a,$$

where μ and $\eta < 1$ are user-defined parameters. To stop the algorithm, we use the following stopping criterion: we stop when

$$|\xi_k^{(l+1)} - \xi_k^{(l)}| \leq \tau_r |\xi_k^{(1)} - \xi_k^{(0)}|,$$

where τ_r is a user-defined parameter.

https://doi.org/10.1051/cocv/2010049 Published online by Cambridge University Press

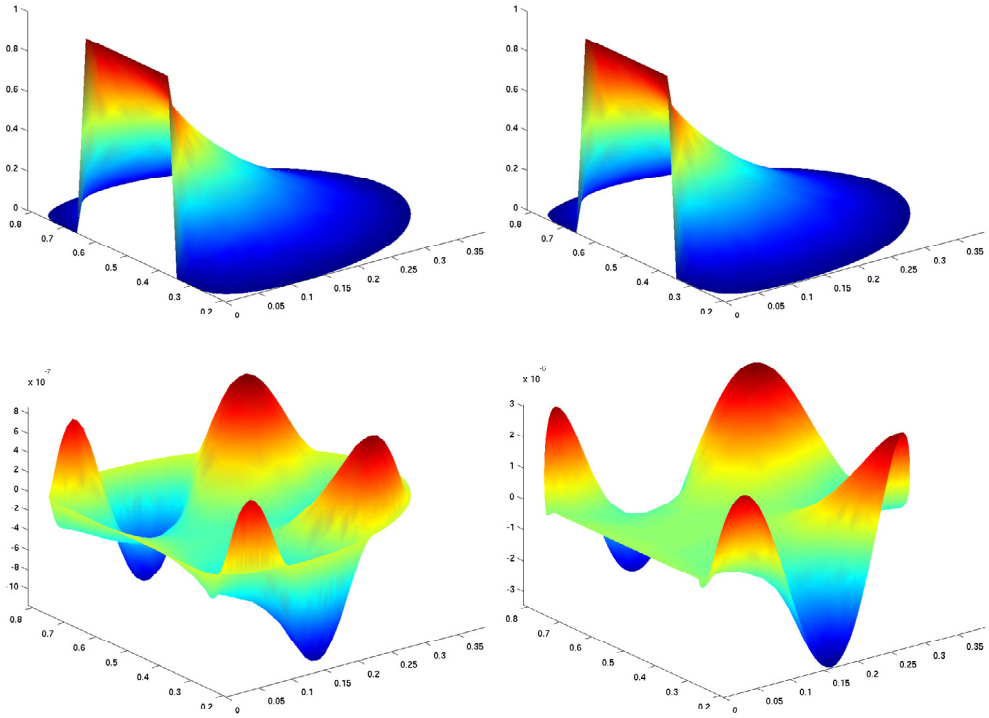


FIGURE 5. Solutions u_1 (top left), $u_{2,\varepsilon}$ (top right), p_1 (bottom left), p_2 (bottom right) in the optimal domain.

7. Numerical results

For the numerical resolution we take $m = 40$ control points ξ_k. We discretize the interval $[0, 1]$ for the parameterization $x(s)$ using 400 points. The domain K is chosen as

$$K = \{0\} \times [0.5 - \kappa_1, 0.5 + \kappa_1],$$

with $\kappa_1 \approx 0.129$. The initial domain L is chosen as

$$L = \{0\} \times [0.5 - \kappa_2, 0.5 - \kappa_1] \cup [0.5 + \kappa_1, 0.5 + \kappa_2],$$

with $\kappa_2 \approx 0.233$. We use the Matlab PDE toolbox to produce a grid in Ω and solve $u_1, u_{2,\varepsilon}, p_1, p_2$ using finite elements. The geometric quantities such as tangent, normal and curvature are computed using (6.3)–(6.4), (6.6) and (6.8), respectively. We initialize the points ξ_k by placing them evenly on a half-circle of center $\{0\} \times \{0.5\}$ and radius 0.3, except for the two first ξ_0, ξ_1 and two last points ξ_{m-1}, ξ_m which have to lay on the axis $\{x_1 = 0\}$ as mentioned earlier. We choose $\mu = 10$, $\eta = 0.5$ for the line search and $\tau_r = 5 \times 10^{-4}$ for the stopping criterion. For the penalization we use (4.17) and choose $\varepsilon = 10^{-1}$ and $q = 4$.

The algorithm terminated after 220 iterations. The results are given in Figures 5 to 7. In Figure 5, the two states u_1 and $u_{2,\varepsilon}$ as well as the two adjoint states p_1 and p_2 are plotted. The difference between u_1 and $u_{2,\varepsilon}$ in the final domain Ω_{final} is plotted in Figure 6, along with the residual $J_\varepsilon(\Omega)$ given by (4.31). In Figure 7, the initial and final boundaries are plotted in blue and red, respectively, while the set of control points of the curve Γ is plotted in green. We observe that the optimal domain is symmetric as expected from Section 3.1.

https://doi.org/10.1051/cocv/2010049 Published online by Cambridge University Press

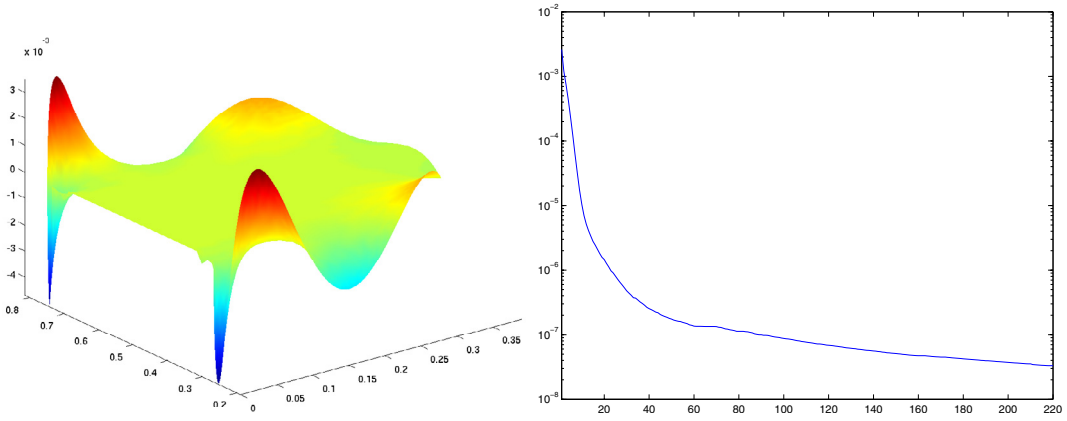


FIGURE 6. Difference $u_1 - u_2$ in the optimal domain (left), residual J_ε (right).

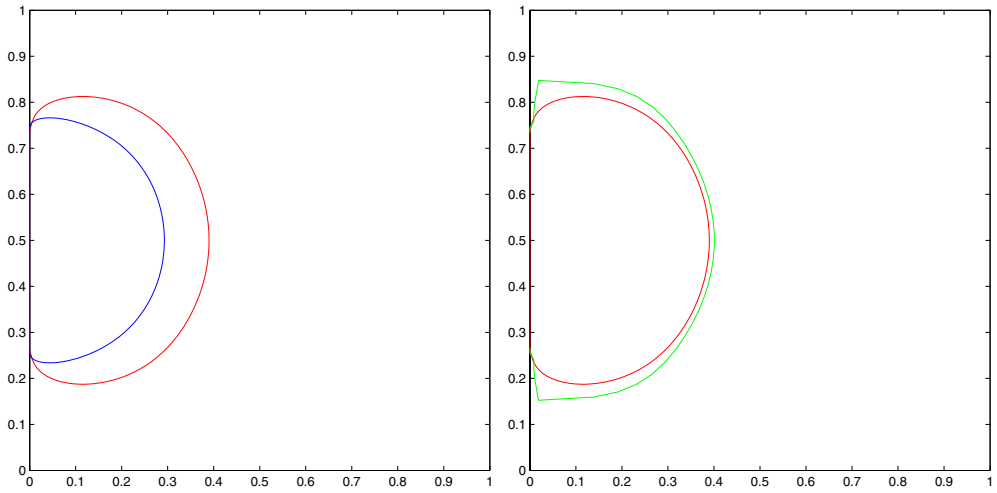


FIGURE 7. Final boundary Γ (red), initial boundary Γ (blue), control points (green). (Figure in color available online at www.esaim-cocv.org.)

The optimal set L_{final} is given by

$$L_{\text{final}} = \{0\} \times [0.5 - \kappa_{fi}, 0.5 - \kappa_1] \cup [0.5 + \kappa_1, 0.5 + \kappa_{fi}]$$

with $\kappa_{fi} \approx 0.2342$. The value of J_ε on the initial domain is

$$J_\varepsilon(\Omega_{\text{initial}}) \approx 2.6 \times 10^{-3},$$

and the value of J_ε on the final domain is

$$J_\varepsilon(\Omega_{\text{final}}) \approx 3.3 \times 10^{-8},$$

as may be seen in Figure 6. Therefore, the shape functional J_ε has been significantly decreased and is close to its global optimum.

https://doi.org/10.1051/cocv/2010049 Published online by Cambridge University Press

Acknowledgements. The authors would like to express a great deal of gratitude to Professor Michel Pierre for several light brighting discussions. The authors further acknowledge financial support by the Austrian Ministry of Science and Education and the Austrian Science Foundation FWF under START-grant Y305 "Interfaces and free boundaries". The second author were partially supported by the ANR project GAOS "Geometric analysis of optimal shapes".

References

[1] A. Acker, An extremal problem involving current flow through distributed resistance. *SIAM J. Math. Anal.* **12** (1981) 169–172.
[2] C. Atkinson and C.R. Champion, Some boundary-value problems for the equation $\nabla \cdot (|\nabla\varphi|^N \nabla\varphi) = 0$. *Quart. J. Mech. Appl. Math.* **37** (1984) 401–419.
[3] A. Beurling, *On free boundary problems for the Laplace equation*, *Seminars on analytic functions* **1**. Institute for Advanced Studies, Princeton (1957).
[4] F. Bouchon, S. Clain and R. Touzani, Numerical solution of the free boundary Bernoulli problem using a level set formulation. *Comput. Methods Appl. Mech. Eng.* **194** (2005) 3934–3948.
[5] E.N. Dancer and D. Daners, Domain perturbation for elliptic equations subject to Robin boundary conditions. *J. Differ. Equ.* **138** (1997) 86–132.
[6] M.C. Delfour and J.-P. Zolésio, *Shapes and geometries – Analysis, differential calculus, and optimization*, *Advances in Design and Control* **4**. Society for Industrial and Applied Mathematics (SIAM), Philadelphia (2001).
[7] L.C. Evans, *Partial differential equations*, *Graduate Studies in Mathematics* **19**. American Mathematical Society, Providence (1998).
[8] A. Fasano, Some free boundary problems with industrial applications, in *Shape optimization and free boundaries (Montreal, PQ, 1990)*, *NATO Adv. Sci. Inst. Ser. C Math. Phys. Sci.* **380**, Kluwer Acad. Publ., Dordrecht (1992) 113–142.
[9] M. Flucher and M. Rumpf, Bernoulli's free boundary problem, qualitative theory and numerical approximation. *J. Reine Angew. Math.* **486** (1997) 165–204.
[10] A. Friedman, Free boundary problem in fluid dynamics, in *Variational methods for equilibrium problems of fluids, Trento 1983*, *Astérisque* **118** (1984) 55–67.
[11] A. Friedman, Free boundary problems in science and technology. *Notices Amer. Math. Soc.* **47** (2000) 854–861.
[12] P. Grisvard, *Elliptic problems in nonsmooth domains*, *Monographs and Studies in Mathematics* **24**. Pitman (Advanced Publishing Program), Boston (1985).
[13] J. Haslinger, T. Kozubek, K. Kunisch and G. Peichl, Shape optimization and fictitious domain approach for solving free boundary problems of Bernoulli type. *Comp. Optim. Appl.* **26** (2003) 231–251.
[14] J. Haslinger, K. Ito, T. Kozubek, K. Kunisch and G. Peichl, On the shape derivative for problems of Bernoulli type. *Interfaces in Free Boundaries* **11** (2009) 317–330.
[15] A. Henrot and M. Pierre, *Variation et optimisation de formes – Une analyse géométrique*, *Mathématiques & Applications* **48**. Springer, Berlin (2005).
[16] A. Henrot and H. Shahgholian, Existence of classical solutions to a free boundary problem for the p-Laplace operator. I. The exterior convex case. *J. Reine Angew. Math.* **521** (2000) 85–97.
[17] A. Henrot and H. Shahgholian, Existence of classical solutions to a free boundary problem for the p-Laplace operator. II. The interior convex case. *Indiana Univ. Math. J.* **49** (2000) 311–323.
[18] A. Henrot and H. Shahgholian, The one phase free boundary problem for the p-Laplacian with non-constant Bernoulli boundary condition. *Trans. Amer. Math. Soc.* **354** (2002) 2399–2416.
[19] K. Ito, K. Kunisch and G.H. Peichl, Variational approach to shape derivatives for a class of Bernoulli problems. *J. Math. Anal. Appl.* **314** (2006) 126–149.
[20] C.T. Kelley, *Iterative methods for optimization*, *Frontiers in Applied Mathematics* **18**. Society for Industrial and Applied Mathematics (SIAM), Philadelphia (1999).
[21] V.A. Kondrat′ev, Boundary value problems for elliptic equations in domains with conical or angular points. *Trudy Moskov. Mat. Obšč.* **16** (1967) 209–292.
[22] C.M. Kuster, P.A. Gremaud and R. Touzani, Fast numerical methods for Bernoulli free boundary problems. *SIAM J. Sci. Comput.* **29** (2007) 622–634.
[23] J. Lamboley and A. Novruzi, Polygons as optimal shapes with convexity constraint. *SIAM J. Control Optim.* **48** (2009) 3003–3025.
[24] E. Lindgren and Y. Privat, A free boundary problem for the Laplacian with a constant Bernoulli-type boundary condition. *Nonlinear Anal.* **67** (2007) 2497–2505.
[25] J. Nocedal and S.J. Wright, *Numerical optimization*. Springer Series in Operations Research and Financial Engineering, Springer, New York, 2nd edition (2006).
[26] J.R. Philip, n-diffusion. *Austral. J. Phys.* **14** (1961) 1–13.
[27] J. Sokołowski and J.-P. Zolésio, *Introduction to shape optimization: Shape sensitivity analysis*, *Springer Series in Computational Mathematics* **16**. Springer-Verlag, Berlin (1992).

https://doi.org/10.1051/cocv/2010049 Published online by Cambridge University Press